

Horizons cannot save the landscapeIosif Bena,^{1,*} Alex Buchel,^{2,3,†} and Óscar J. C. Dias^{1,‡}¹*Institut de Physique Théorique, CEA Saclay, CNRS URA 2306, F-91191 Gif-sur-Yvette, France*²*Department of Applied Mathematics, University of Western Ontario, London, Ontario N6A 5B7, Canada*³*Perimeter Institute for Theoretical Physics, Waterloo, Ontario N2J 2W9, Canada*

(Received 16 January 2013; published 28 March 2013)

Solutions with anti-D3 branes in a Klebanov-Strassler geometry with positive charge dissolved in fluxes have a certain singularity corresponding to a diverging energy density of the Ramond-Ramond and Neveu-Schwarz-Neveu-Schwarz three-form fluxes. There are many hopes and arguments for and against this singularity, and we attempt to settle the issue by examining whether this singularity can be cloaked by a regular event horizon. This is equivalent to the existence of asymptotically Klebanov-Tseytlin or Klebanov-Strassler black holes whose charge measured at the horizon has the opposite sign to the asymptotic charge. We find that no such Klebanov-Tseytlin solution exists. Furthermore, for a large class of Klebanov-Strassler black holes we considered, the charge at the horizon must also have the same sign as the asymptotic charge and is completely determined by the temperature, the number of fractional branes and the gaugino masses of the dual gauge theory. Our result suggests that antibrane singularities in backgrounds with charge in the fluxes are unphysical, which in turn raises the question as to whether antibranes can be used to uplift anti-de Sitter vacua to deSitter ones. Our results also point to a possible instability mechanism for the antibranes.

DOI: [10.1103/PhysRevD.87.063012](https://doi.org/10.1103/PhysRevD.87.063012)

PACS numbers: 97.60.Lf, 11.25.Tq

I. INTRODUCTION

The backreaction of antibranes in backgrounds with charge dissolved in fluxes, like the Klebanov-Strassler (KS) [1] and the Klebanov-Tseytlin (KT) solutions [2], has been a subject of intense study over the past few years. A probe analysis of anti-D3 branes in the KS solution reveals that these branes have a nontrivial potential that drives them to polarize into NS5-branes, wrapping a two-sphere inside the large three-sphere at the KS tip [3]. On the other hand, if one tries to go beyond the probe approximation and obtain the backreacted solution corresponding to smeared anti-D3 branes at the tip of the KS solution, a surprise awaits: both the first-order backreacted solution [4–7] as well as the fully backreacted solution [8] have a singularity.

The fate of this singularity is crucial. Adding anti-D3 branes to a KS-like throat is the most generic way to uplift the vacuum energy of the AdS vacua that come out of string theory flux compactifications with stabilized moduli [9] and obtain deSitter vacua. If the singularity of the anti-D3 solution is not physical, this implies that anti-D3 branes cannot be used to give KS metastable vacua and to uplift the AdS vacua to dS. Since the other known uplift mechanisms (such as F- or D-term uplifting [10,11] or Kähler uplifting [12,13]) are much less generic, this would imply that string theory does not have a landscape of dS vacua. Thus the fate of this singularity is closely intertwined with that of the landscape.

In both the first-order and the fully backreacted solution, this singularity comes from three-form RR and Neveu-Schwarz-Neveu-Schwarz field strengths whose energy densities diverge. There have been quite a few arguments both in favor and against this singularity. The arguments in favor of this singularity [14] are based on the self-consistency of the probe approximation of Ref. [3] and on the fact that the divergent energy of the singularity has a finite integral.¹ The arguments against it are that the self-consistency of the probe approximation does not imply the existence of metastable vacua when backreaction is taken into account [15,16]. Furthermore, the finiteness of the integral of the divergent energy density near a singularity can hardly constitute a criterion for accepting it: the negative-mass Schwarzschild solution also has a singularity with finite energy, and yet has to be discarded as unphysical [17].²

It has also been argued that this singularity signals the tendency of the branes to polarize (as it happens in the probe approximation [3]), and one can therefore hope that this singularity could be resolved by brane polarization [21] à la Polchinski-Strassler [22]. However, the recent calculation of [23]³ pours cold water on this hope: neither the smeared anti-D3 branes nor the localized ones polarize into D5 branes, wrapping the S^2 of the warped deformed conifold

¹In Ref. [14] it was also argued that the singularity may be an artifact of first-order backreaction, but this has been shown not to happen [8].

²Furthermore, there are similar singularities near anti-M2 [18,19] and anti-D2 branes [20], and for those singularities both the energy density and its integral diverge.

³As well as the earlier analysis of anti-D6 singularities [24–27].

*iosif.bena@cea.fr

†abuchel@perimeterinstitute.ca

‡oscar.dias@cea.fr

at a finite distance away from the KS tip despite the fact that *all* the terms of the Polchinski-Strassler polarization potential are there. Since in Polchinski-Strassler there are always multiple channels for brane polarization, the absence of a D5 brane polarization channel for localized branes suggests that the NS5 channel found in a brane probe approximation in Ref. [3] is also not present in the backreacted solution.

Given that all the calculations made so far that could have either confirmed or invalidated the arguments in favor of this singularity have given negative results, the main hope left is that some hither unknown physical phenomenon will come to its rescue and resolve it. Even if this “resolution by mystery” proposal has not yet been articulated, it does appear to us that disproving it beforehand might once and for all settle the discussion.

The clearest argument that a given unknown singularity can be physical has been formulated by Gubser in Ref. [28], who argued that if the singularity can be cloaked by an event horizon it is physical, and conversely if a singularity cannot be obtained by “turning off” a black hole horizon, then it is not physical. Hence, if the anti-D3 singularity were physical, one would expect that there should exist a black hole in Klebanov-Strassler and/or Klebanov-Tseytlin whose charge has the opposite sign to the charge dissolved in the fluxes.

Our purpose is to revisit the KT and KS black holes constructed numerically in the past and to show that no such black holes exist. The existence of the Klebanov-Tseytlin black hole solution was first proposed in Ref. [29] and then was constructed in perturbation theory around the black hole in Klebanov-Witten [30] in Refs. [31,32]. However, the equations underlying the nonlinear solution cannot be solved analytically, and the full solution was constructed numerically in Refs. [33–35].⁴ Interestingly enough, extending the ansatz to describe black holes in Klebanov-Strassler is not so hard, but it turns out that these solutions (which would be dual to a deconfined phase with spontaneously broken chiral symmetry) do not exist [38]! The only way to build a black hole in Klebanov-Strassler is to turn on one or two non-normalizable modes corresponding to gaugino masses in the dual theory, which break explicitly the chiral symmetry [38].

In this paper we review the one-parameter family of KT black holes and the three-parameter family of mass-deformed KS black holes, and we calculate the D3 charge at the horizon. We find that this charge does not have an opposite sign to the asymptotic charge of the solution. In fact, for a KT black hole of a given temperature, the value of this charge is not a free parameter, as one might expect naively from the perturbative analysis of Ref. [32]. Hence, if one imagines keeping the temperature fixed and lowering probe charges into the black hole, the configuration will

settle back to the original charge. This comes essentially because the KT solution has charge dissolved in the fluxes, and an over-charged or an under-charged black hole can expel or absorb charge from the surrounding charge in the fluxes to bring back its charge to its initial value. A similar story happens for the mass-deformed KS black hole: if one adds positive or negative charge to the black hole keeping the temperature and gaugino masses fixed, the black hole will interact with the surrounding flux and return to its original charge.

In Sec. II we discuss the KT black hole and examine the symmetries of the background, the single-parameter nature of the solution and the relationship between its temperature and the charge. In Sec. III we explore in more detail the three-parameter mass-deformed KS black hole of Ref. [38] and explain the relation between gaugino masses, temperature and charge. We conclude with a few comments and suggestions for future work in Sec. IV.

II. THE KLEBANOV-TSEYTLIN BLACK HOLE

A. The cascading gauge theory and its chiral symmetric phases

The $\mathcal{N} = 1$ supersymmetric $SU(N) \times SU(N + M)$ cascading gauge theory can be realized as the world-volume theory on N regular D3 branes to which we add M fractional D3 branes (wrapped D5 branes) to the apex of the conifold singularity. At low temperatures this cascading gauge theory spontaneously breaks a discrete chiral symmetry, which corresponds in the dual bulk to the deformation of the conifold singularity. The full warped deformed conifold solution dual to this cascading gauge theory was constructed by Klebanov and Strassler (KS) in Ref. [1]. One can also construct a singular solution dual to the chirally symmetric phase of this theory (the Klebanov-Tseytlin (KT) solution [2]). The two solutions have D3 brane charges dissolved in the fluxes.

This cascading gauge theory is an ideal testing ground for understanding the deconfinement phase transition of strongly coupled QCD-like gauge theories. The KS solution is holographically dual to the confined chiral-symmetry-broken phase, and the high temperature deconfined phase with unbroken chiral symmetry was argued in Ref. [29] to be dual to a black hole added to the KT solution. This black hole was constructed in a perturbative expansion [31–33,35] in the fractional brane number M around the black hole in Klebanov-Witten [30] and then at full nonlinear level in Refs. [34,35], using numerical methods.

We will review this solution, highlighting properties that are relevant for our study. We emphasize that this is a one-parameter of solutions, and we show that this black hole will always have positive Maxwell D3 brane charge at the horizon. Hence, there are no KT black hole solutions with anti-D3 brane charge, contrary to what one might have expected from the perturbative story.

⁴Other attempts to construct such black holes were discussed in Refs. [36,37].

B. The Klebanov-Tseytlin black hole

We review the construction of the Klebanov-Tseytlin black hole, which is a solution of ten-dimensional type IIB supergravity that asymptotes to the Klebanov-Tseytlin (KT) background [2] and is holographically dual to a high-temperature deconfined chirally symmetric phase of the cascading gauge theory. Recall that the IIB supergravity field content includes, besides the gravitational field, a dilaton $\Phi = \ln g$, a Neveu-Schwarz-Neveu-Schwarz flux $H_3 = dB_2$, and Ramond-Ramond fluxes F_3 and F_5 (the axion vanishes, $C_0 = 0$). These solutions have a Z_{2M} chiral symmetry, a $U(1)_B$ symmetry and a $SU(2) \times SU(2)$ global symmetry. In the absence of the black hole, the KT background is a direct product of \mathcal{M}_5 with metric $g_{\mu\nu}$ and a squashed $T^{1,1}$ with the radii of curvature of \mathcal{M}_5 and the fluxes H_3 , F_5 varying logarithmically in the radial coordinate.

The most general ansatz (in the Einstein frame) that is a deformation of the KT background [2] which preserves its $SU(2) \times SU(2) \times \mathbb{Z}_{2P} \times U(1)_B$ symmetry is [33,34],

$$\begin{aligned} ds_{10}^2 &= g_{\mu\nu}(y)dy^\mu dy^\nu + ds_{T^{1,1}}^2, \\ ds_{T^{1,1}}^2 &= \Omega_1^2(y)e_\psi^2 + \Omega_2^2(y) \sum_{a=1}^2 (e_{\theta_a}^2 + e_{\phi_a}^2), \end{aligned} \quad (2.1)$$

and (we set $\alpha' \equiv 1$)

$$\begin{aligned} F_3 &= P e_\psi \wedge (e_{\theta_1} \wedge e_{\phi_1} - e_{\theta_2} \wedge e_{\phi_2}), \\ B_2 &= \frac{K(y)}{2P} (e_{\theta_1} \wedge e_{\phi_1} - e_{\theta_2} \wedge e_{\phi_2}), \\ F_5 &= \mathcal{F}_5 + \star \mathcal{F}_5, \\ \mathcal{F}_5 &= -K(y) e_\psi \wedge e_{\theta_1} \wedge e_{\phi_1} \wedge e_{\theta_2} \wedge e_{\phi_2}, \end{aligned} \quad (2.2)$$

where y denotes the coordinates of \mathcal{M}_5 (greek indices μ, ν run from 0 to 4) and $ds_{T^{1,1}}^2$ is the line element of the

warp-squashed $T^{1,1}$, with the one-forms $e_\psi, e_{\theta_a}, e_{\phi_a}$ ($a = 1, 2$) given by

$$\begin{aligned} e_\psi &= \frac{1}{3} \left(d\psi + \sum_{a=1}^2 \cos \theta_a d\phi_a \right), \quad e_{\theta_a} = \frac{1}{\sqrt{6}} d\theta_a, \\ e_{\phi_a} &= \frac{1}{\sqrt{6}} \sin \theta_a d\phi_a. \end{aligned} \quad (2.3)$$

The range of the $T^{1,1}$ coordinates is $0 \leq \psi \leq 4\pi$, $0 \leq \theta_a \leq \pi$ and $0 \leq \phi_a \leq 2\pi$. The dimensionful constant P in (2.2) is related to the quantized dimensionless units of flux M entering in the rank of the gauge groups of the dual field theory. We work in the normalization, where

$$P = \frac{3}{2^{3/4} \pi} G_5^{1/4} M, \quad (2.4)$$

where $G_5 = G_{10}/\text{vol}_{T^{1,1}}$ is the five-dimensional Newton's constant obtained after the dimensional reduction on $T^{1,1}$ done next.

With this ansatz, we can do a standard Kaluza-Klein reduction of the type IIB action to five dimensions and get the effective action [33],

$$\begin{aligned} S_5 &= \frac{1}{16\pi G_5} \int_{\mathcal{M}_5} \text{vol}_{\mathcal{M}_5} \left\{ \Omega_1 \Omega_2^4 \left(R_{10} - \frac{1}{2} \nabla_\mu \Phi \nabla^\mu \Phi \right) \right. \\ &\quad \left. - P^2 \Omega_1 e^{-\Phi} \left(\frac{\nabla_\mu K \nabla^\mu K}{4P^4} + \frac{e^{2\Phi}}{\Omega_1^2} \right) - \frac{1}{2} \frac{K^2}{\Omega_1 \Omega_2^4} \right\}, \end{aligned} \quad (2.5)$$

where R_{10} is the ten-dimensional Ricci scalar related to the five-dimensional Ricci scalar R_5 by

$$\begin{aligned} R_{10} &= R_5 - 2\Omega_1^{-1} g^{\lambda\nu} (\nabla_\lambda \nabla_\nu \Omega_1) - 8\Omega_2^{-1} g^{\lambda\nu} (\nabla_\lambda \nabla_\nu \Omega_2) \\ &\quad - 4g^{\lambda\nu} (2\Omega_1^{-1} \Omega_2^{-1} \nabla_\lambda \Omega_1 \nabla_\nu \Omega_2 \\ &\quad + 3\Omega_2^{-2} \nabla_\lambda \Omega_2 \nabla_\nu \Omega_2) + 24\Omega_2^{-2} - 4\Omega_1^2 \Omega_2^{-4}. \end{aligned} \quad (2.6)$$

The associated equations of motion are [33]

$$\begin{aligned} 0 &= \frac{1}{\sqrt{-g}} \partial_\mu \left[\frac{e^{-\Phi} \Omega_1}{2P^2} \sqrt{-g} g^{\mu\nu} \partial_\nu K \right] - \frac{K}{\Omega_1 \Omega_2^4}, & 0 &= \frac{1}{\sqrt{-g}} \partial_\mu \left[\Omega_1 \Omega_2^4 \sqrt{-g} g^{\mu\nu} \partial_\nu \Phi \right] + \frac{\Omega_1 e^{-\Phi} (\partial K)^2}{4P^2} - \frac{P^2 e^\Phi}{\Omega_1}, \\ 0 &= \Omega_2^4 R_5 - 12\Omega_2^2 (\partial \Omega_2)^2 + 24\Omega_2^2 - 12\Omega_1^2 - 8\Omega_2^3 \square_5 \Omega_2 - \frac{1}{2} \Omega_2^4 (\partial \Phi)^2 + \frac{P^2 e^\Phi}{\Omega_1^2} - \frac{e^{-\Phi} (\partial K)^2}{4P^2} + \frac{K^2}{2\Omega_1^2 \Omega_2^4}, \\ 0 &= 4\Omega_1 \Omega_2^3 R_5 - 8\Omega_2^3 \square_5 \Omega_1 - 24\Omega_1 \Omega_2^2 \square_5 \Omega_2 - 24\Omega_2^2 \partial \Omega_1 \partial \Omega_2 - 24\Omega_1 \Omega_2 (\partial \Omega_2)^2 + 48\Omega_1 \Omega_2 - 2\Omega_1 \Omega_2^3 (\partial \Phi)^2 \\ &\quad + \frac{2K^2}{\Omega_1 \Omega_2^5}, \\ \Omega_1 \Omega_2^4 R_{5\mu\nu} &= \frac{g_{\mu\nu}}{3} \left[\frac{P^2 e^\Phi}{\Omega_1} + \frac{K^2}{2\Omega_1 \Omega_2^4} + \square_5 (\Omega_1 \Omega_2^4) - 24\Omega_1 \Omega_2^2 + 4\Omega_1^3 \right] + \nabla_\mu \nabla_\nu (\Omega_1 \Omega_2^4) - 4\Omega_2^3 (\partial_\mu \Omega_1 \partial_\nu \Omega_2 + \partial_\nu \Omega_1 \partial_\mu \Omega_2) \\ &\quad - 12\Omega_1 \Omega_2^2 \partial_\mu \Omega_2 \partial_\nu \Omega_2 + \frac{\Omega_1 e^{-\Phi}}{4P^2} \partial_\mu K \partial_\nu K + \frac{1}{2} \Omega_1 \Omega_2^4 \partial_\mu \Phi \partial_\nu \Phi, \end{aligned} \quad (2.7)$$

where $(\partial F)^2$ denotes $g^{\mu\nu} \partial_\mu F \partial_\nu F$ and \square_5 is the Laplacian in \mathcal{M}_5 .

An ansatz for the \mathcal{M}_5 gravitational field that is tailored to search for the KT black hole with horizon located at $x = 1$ and asymptotic KT background at $x \rightarrow 0$ is [34]

$$ds_{\mathcal{M}_5}^2 = h^{-1/2}(2x-x^2)^{-1/2}[-(1-x)^2 dt^2 + dx_1^2 + dx_2^2 + dx_3^2] + G_{xx} dx^2, \quad (2.8)$$

and it is also useful to rewrite the squashed $T^{1,1}$ factors as

$$\Omega_1 = h^{1/4} \sqrt{f_2}, \quad \Omega_2 = h^{1/4} \sqrt{f_3}. \quad (2.9)$$

In these expressions, h , f_2 , f_3 , G_{xx} are functions of the compact radial coordinate x . Recall that the solution is fully specified once we find in addition the dilaton $\Phi = \ln g(x)$ and flux forms (2.2), which are determined by a single function $K(x)$.

In these conditions, it follows from the equations of motion (2.7) that G_{xx} is given by an algebraic relation that is a function of $\{h, f_2, f_3, K, g\}$ and their first derivatives. So, in total, to determine our black hole we need to solve a system of five second-order coupled and nonlinear ODEs for $\{h, f_2, f_3, K, g\}$. The explicit algebraic relation for G_{xx} and the system of five equations of motion are explicitly written in equations (2.6)–(2.12) of Ref. [34]. An important observation is that each of these five equations is second order. Therefore, the total differential order of the system is 10.

To find the KT black hole we solve the equations of motion subject to appropriate boundary conditions at the horizon, $x \rightarrow 1$, and at the asymptotic boundary, $x \rightarrow 0$.

The IR boundary condition (horizon) is quite standard in black hole physics. Formally, we rewrite our ansatz in ingoing Eddington-Finkelstein coordinates (appropriate to extend the analysis through the horizon), and we require regularity of all our fields at the horizon in this coordinate system. This amounts to saying that all our functions must have a series expansion in $(1-x)^2$ [34],

$$\begin{aligned} h &= \sum_{n=0}^{\infty} h_n^h (1-x)^{2n}, & f_2 &= \sum_{n=0}^{\infty} a_n^h (1-x)^{2n}, \\ f_3 &= \sum_{n=0}^{\infty} b_n^h (1-x)^{2n}, & g &= \sum_{n=0}^{\infty} g_n^h (1-x)^{2n}, \\ K &= \sum_{n=0}^{\infty} k_n^h (1-x)^{2n}, \end{aligned} \quad (2.10)$$

with the boundary condition simply requiring that the coefficients $\{h_0^h, a_0^h, b_0^h, k_0^h, g_0^h\}$ are constants. Solving the five equations of motion perturbatively around the horizon up to arbitrary order, one finds that only a few of the coefficients in (2.10) are independent, with all the others being a function of these. Concretely, one chooses the six IR independent parameters to be

$$\text{IR independent parameters (6): } \{h_0^h, a_0^h, b_0^h, k_0^h, g_0^h, a_1^h\}. \quad (2.11)$$

Consider now the UV asymptotic structure at $x \rightarrow 0$. The UV boundary condition is straightforward: we want the KT black hole to approach asymptotically the KT solution [2]. The latter is the leading-order contribution of a power series expansion in x and $\ln(x)$ of the equations of motion [34],

$$\begin{aligned} h &= h_0 - \frac{P^2 g_0}{8a_0^2} \ln(x) + \sum_{n=1}^{\infty} \sum_{k=1}^{n-1} h_{n,k} x^{n/2} \ln^k(x), \\ f_2 &= a_0 + \sum_{n=1}^{\infty} \sum_{k=1}^{n-1} a_{n,k} x^{n/2} \ln^k(x), \\ f_3 &= a_0 + \sum_{n=1}^{\infty} \sum_{k=1}^{n-1} b_{n,k} x^{n/2} \ln^k(x), \\ g &= g_0 + \sum_{n=1}^{\infty} \sum_{k=1}^{n-1} g_{n,k} x^{n/2} \ln^k(x) \\ K &= 4h_0 a_0^2 - \frac{1}{2} P^2 g_0 - \frac{1}{2} P^2 g_0 \ln(x) + \sum_{n=1}^{\infty} \sum_{k=1}^{n-1} K_{n,k} x^{n/2} \ln^k(x). \end{aligned} \quad (2.12)$$

The presence of the $\ln x$ terms in h , K in the KT leading contribution is responsible for the logarithmic running of the fluxes and \mathcal{M}_5 radii of curvature.

As expected, not all coefficients in the expansion (2.12) are independent. There are four independent asymptotic parameters already present in the KT solution and those we choose to be $\{P, g_0, a_0, h_0\}$. P is related to the quantized flux M by (2.4), g_0 is related to the dimensionless parameter of the cascading gauge theory, and there are two combinations of the other two parameters that are related to the temperature and dynamical scale of the cascading gauge theory. More concretely, one has $a_0^2 = 4\pi G_5 s T$, where s and T are the entropy density and temperature of the solution, which can be computed directly from the horizon area and surface gravity using the expansion (2.10). In addition, we can replace the independent parameter h_0 by a new dimensionless parameter k_s defined as

$$k_s \equiv \frac{4h_0 a_0^2}{P^2 g_0} - \frac{1}{2} \equiv \frac{1}{2} \ln \left(\frac{4\pi G_5 s T}{\Lambda^4} \right). \quad (2.13)$$

This relation defines the dynamical scale Λ of the cascading theory. The other UV independent coefficients correspond to vacuum expectation values (VEVs) of the operators dual to the fields for which we are solving. After using the conformal anomaly equation [33], one finds that there are four VEV independent parameters, chosen to be $\{a_{2,0}, g_{2,0}, a_{3,0}, a_{4,0}\}$.

We conclude that there are eight UV independent parameters that determine the coefficients in (2.12) to any order we wish. These can be chosen to be $\{P, g_0, a_0, k_s, a_{2,0}, g_{2,0}, a_{3,0}, a_{4,0}\}$. We can, however, use the symmetries of the problem to get rid of some of these parameters. First, observe that the ansatz (2.8) is invariant under the scaling symmetry,⁵

⁵This scaling symmetry leaves $h_0 a_0^2$ invariant. This means that $h_0 a_0^2$ is a function of the dimensionless parameter of our theory, which is the ratio between the temperature and the dynamical scale Λ . This motivates the definition (2.13).

$$\begin{aligned} (t, x, \vec{x}) &\rightarrow (\lambda^{-2}t, x, \lambda^{-2}\vec{x}), & h &\rightarrow \lambda^{-2}h, \\ f_{2,3} &\rightarrow \lambda f_{2,3}, & g &\rightarrow g & K &\rightarrow K. \end{aligned} \quad (2.14)$$

We use this scaling symmetry to set $a_0 \equiv 1$. In addition, we are working in the supergravity approximation (where we neglect g_s and α' corrections). In this approximation, the action and the associated equations of motion do not depend separately on P^2 and g_0 but only on the combination $P^2 g_0$. We can thus set $g_0 \equiv 1$. Furthermore, when we neglect α' corrections, the action is multiplied by a constant when we rescale the ten-dimensional metric by a constant factor (and rescale the p forms accordingly), so that the equations of motion are left invariant. This transformation acts on our variables as

$$\begin{aligned} h &\rightarrow \lambda^{-2}h, & f_{2,3} &\rightarrow \lambda^2 f_{2,3}, & K &\rightarrow \lambda^2 K, \\ g &\rightarrow g, & P &\rightarrow \lambda P. \end{aligned} \quad (2.15)$$

As long as we work in the supergravity approximation, we can thus use this symmetry to set $P \equiv 1$ and use the scaling (2.15) to generate the solutions for any other value of P .

To sum, after using the symmetries of our system we find that we are left with five independent UV parameters,

$$\text{UV independent parameters (5): } \{k_s, a_{2,0}, g_{2,0}, a_{3,0}, a_{4,0}\}. \quad (2.16)$$

At this point we can ask how many parameters we need to describe the KT black hole solution. We have a total of $6 + 5 = 11$ IR and UV independent parameters (2.11) and (2.16), and the equations of motion are a system of total differential order 10. We thus conclude that the KT black hole is a one-parameter family of solutions. In the numerical search of the KT black hole, we will take this dimensionless parameter to be k_s . Equation (2.13) can then be used to translate the results we obtain in terms of the dimensionless temperature T/Λ .

The black hole is constructed numerically using a standard shooting method. One fixes the microscopic free parameter of the theory, k_s , and wants to find the other ten IR and UV independent parameters (2.11) and (2.16). The equations of motion have the following two critical points: at the horizon, $x = 1$, and at the boundary, $x = 0$. Consider first the horizon. Using the IR series expansion (2.10), one constructs the solution in the near-horizon region up to the tenth order ($n = 5$ inclusive) in the radial distance to the horizon. This solution depends on the six IR parameters (2.11). One then integrates numerically the six radial second-order ODEs, using a Runge-Kutta method, up to a large radial distance. The procedure is repeated, this time at the asymptotic critical point where one starts by obtaining the asymptotic solution up to ninth order ($n = 9$, inclusive), using the UV series expansion (2.12). Fixing k_s , this asymptotic solution is a function of the four UV parameters $\{a_{2,0}, g_{2,0}, a_{3,0}, a_{4,0}\}$. One integrates this solution down to very small values of the radial distance. In the

overlapping region of the two solutions, we then do their matching, more precisely at $x = 0.5$. The requirement that both the set of five functions $\{h, f_2, f_3, K, g\}$ and their first derivatives must be continuous gives ten conditions that we use to fix the ten IR and UV independent parameters (for a given k_s). The whole process is now repeated for other values of k_s to generate the results that will be presented in the next subsection.

C. Properties of the Klebanov-Tseytlin black hole

We are ready to discuss some physical properties of the Klebanov-Tseytlin black hole that are relevant for our study. For a detailed account of other properties, see Refs. [34,35].

We present the results as a function of either the microscopic parameter k_s (which defines uniquely the solution) or as a function of the dimensionless quantity T/Λ , where T is the temperature of the solution and Λ is the dynamical scale of the theory, related to k_s via (2.13). As explained above, the numerical construction of the solution exploits the scaling symmetries of the theory and is done at $P = g_0 = a_0 \equiv 1$. One can then restore the correct powers of P using the scaling symmetry (2.15), which also introduces a factor of g_0/a_0 together with every factor of P^2 . In order to relax the $a_0 = 1$ condition, we then use (2.13) which implies that all the dimensional quantities must be computed in units of $\Lambda = e^{-k_s/2}$.

From the surface gravity we can compute the black hole temperature, which in Λ units is

$$\frac{T}{\Lambda} = \frac{e^{k_s/2}}{4\pi h_0^h b_0^h} \sqrt{\frac{2(8h_0^h (a_0^h)^2 - g_0^h P^2)}{a_0^h + 2a_1^h}} \quad (2.17)$$

and enables an immediate translation of a dependence on k_s into a dependence on the temperature. The entropy density is computed from the horizon area. The energy density \mathcal{E} and pressure \mathcal{P} of the KT deconfined plasma phase can be read from the expectation values of the appropriate components of the holographic stress tensor T_{ab} , $\mathcal{E} = \langle T_{tt} \rangle$ and $\mathcal{P} = \langle T_{x_i x_i} \rangle$. Moreover, since there are no chemical potentials, the free energy density is simply $\mathcal{F} = -\mathcal{P}$. These quantities are dimensionless if expressed in Λ units and given by

$$\begin{aligned} \frac{4\pi G_5}{P^2 g_0^2} \frac{s}{T^3} &= \left(\frac{T}{\Lambda}\right)^{-4} e^{2k_s}, \\ \frac{32\pi^4}{81} \frac{\mathcal{E}}{\Lambda^4} &= \frac{3}{4} \left(1 + \frac{4}{7} \frac{a_{2,0}}{a_0}\right) e^{2k_s}, \\ \frac{32\pi^4}{81} \frac{\mathcal{F}}{\Lambda^4} &= \frac{3}{7} \left(\frac{a_{2,0}}{a_0} - \frac{7}{12}\right) e^{2k_s}. \end{aligned} \quad (2.18)$$

We can now describe the KT black hole using these thermodynamic quantities. The microscopic parameter k_s has no positive upper bound. For large positive values of k_s , the temperature is large and then decreases as k_s decreases

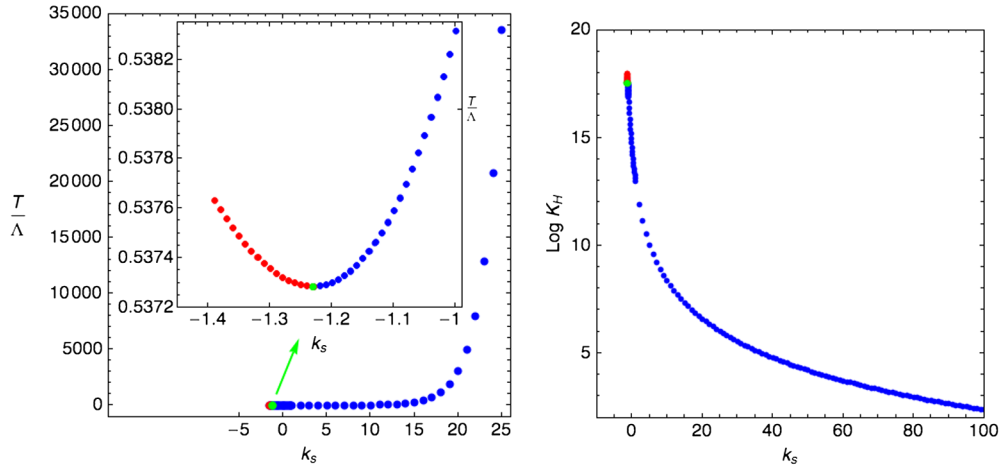


FIG. 1 (color online). *Left Panel:* The dimensionless temperature $\frac{T}{\Lambda}$ as a function of the microscopic parameter k_s . The inset plot zooms it in the neighborhood of $T = T_u$ (green point, i.e., minimum point). The red dots (to the left of the minimum) correspond to $k_s \leq k_u$, and the blue dots (to the right of the minimum) correspond to $k_s \geq k_u$. To the left of the last red dot there are no black holes. *Right Panel:* The Kretschmann scalar at the horizon as a function of the microscopic parameter k_s .

(see left panel of Fig. 1). However, as we keep decreasing k_s , the temperature reaches a minimum at $k_s = k_s^u = -1.230(3)$ (green dot in Fig. 1) and, for even smaller k_s , it increases until a critical lower bound, $k_s = k_s^{\text{crit}}$, is reached (represented by the last numerical red point in Fig. 1). As this critical value is approached, the curvature invariant (like the Kretschmann scalar in the Einstein frame) grows without bound, as shown in the right panel of Fig. 1, which implies that the solution will develop a naked singularity. Below $k_s = k_s^{\text{crit}}$ there are no longer KT black holes. In Fig. 1, the inset plot shows the behavior of the temperature around its minimum value. In all the plots of this section, the numerical red dots describe the region with $k_s \leq k_u$, and the blue dots correspond to $k_s \geq k_u$.

The left panel of Fig. 2 shows what happens to the energy density as a function of the parameter space. For larger temperatures it grows monotonically. On the other hand, the free energy density as a function of the temperature is plotted in the right panel of Fig. 2. For large values of the temperature, the KT black hole solution is the preferred thermodynamic phase since its free energy is negative. However, it vanishes at⁶

$$T_c = 0.6141111(3)\Lambda \quad (2.19)$$

and is positive for smaller temperatures. A first-order deconfinement/confinement phase transition occurs at $T = T_c$ (represented by the magenta point in Fig. 2). The inset plot in this right panel shows how the free energy behaves in the vicinity of $T = T_u$ (green point). We see that in

⁶To pinpoint with higher accuracy the critical temperatures of the green ($T = T_u$) and magenta points ($T = T_c$), we have made runs in the code in a small window around these points with much higher resolution than the one presented in the figures.

this region the free energy stays positive, but precisely at $T = T_u(k_s^u)$ with

$$T_u = 0.8749(0)T_c \quad (2.20)$$

we find a cusp, and a continuous phase transition occurs. To the right of this cusp, and within the temperature window $T_u < T < T(k_s^{\text{crit}})$, we have two phases. The red phase, with $k_s^{\text{crit}} < k < k_s^u$, always has higher free energy for a given temperature. So it is never the thermodynamically preferred phase in the canonical ensemble. Note also that the solution is regular at the cusp (in particular, in the equivalent plot of free energy versus k_s , this cusp corresponds to a maximum inflection point of the curve).

Plotting the dimensionless entropy density $\frac{4\pi G_s}{P^2 g_0^2} \frac{s}{T^3}$ as a function of the dimensionless energy density $\frac{32\pi^4}{81} \frac{\mathcal{E}}{\Lambda^4}$, we find that the two branches of solution can never have the same energy and entropy densities (see left panel of Fig. 2).

So, why is $T = T_u$ so special? The answer relies on the study of the speed of sound waves in the cascading plasma [35]. In the gravitational description, this speed of sound c_s can be computed from the lowest quasinormal mode dispersion relation in the sound channel. Alternatively, in the dual gauge theory description, it is computed from the standard thermodynamic relation $c_s = \sqrt{\frac{\partial P}{\partial \mathcal{E}}}$. It turns out to be

$$c_s^2 = \frac{1}{3} \frac{7 - 12 \frac{a_{2,0}}{a_0} - 6P^2 \frac{da_{2,0}}{dk_s}}{7 + 4 \frac{a_{2,0}}{a_0} + 2P^2 \frac{da_{2,0}}{dk_s}}. \quad (2.21)$$

In the vicinity of $T_u(k_s^u)$ (determined by the condition $c_s = 0$), we find that $c_s \sim (k_s - k_s^u)$ and $c_s \sim (1 - \frac{T_u}{T})^{1/4}$. Thus, the speed of sound becomes imaginary for $k_s < k_s^u$ (red dots), as shown in the right panel of Fig. 3. Consequently, the specific heat $c_V = \frac{s}{c_s^2}$ of the cascading

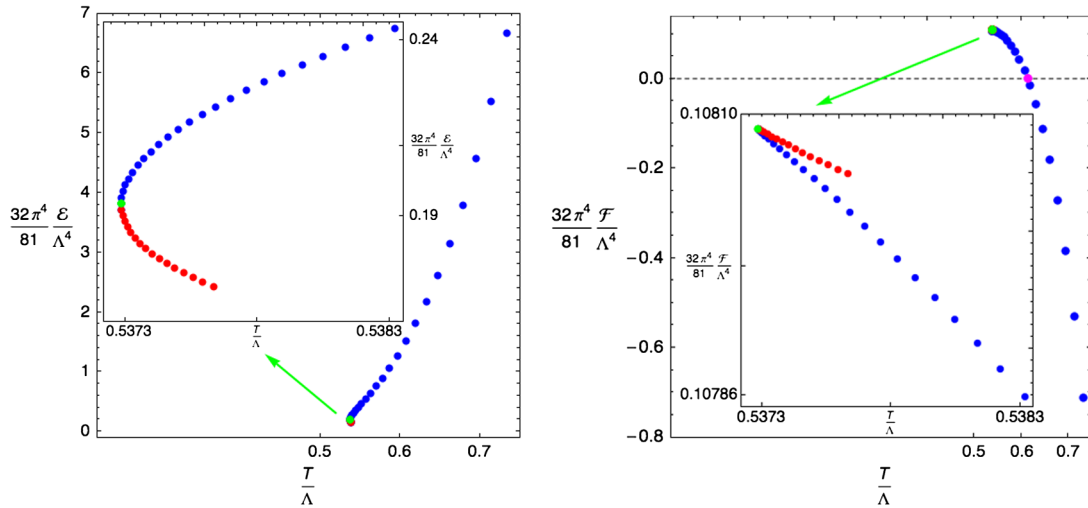


FIG. 2 (color online). *Left Panel:* The dimensionless energy density as a function of the dimensionless temperature. The inset plot shows this energy in the vicinity of the onset of the perturbative instability of the cascading plasma (where $T = T_u$, the green point where the derivative diverges). *Right Panel:* The dimensionless free energy density as a function of the temperature for temperatures at the deconfinement transition ($T = T_c$; magenta point where free energy vanishes) and around it. The inset plot shows the free energy density in the vicinity of the perturbative instability of the cascading plasma ($T = T_u$; green point at the cusp) and all the way down to the last red point in the upper branch that represents the last KT black hole that exists. In these figures, the red/blue dots have the same meaning as in Fig. 1.

plasma diverges at the threshold of the linear instability, $T = T_u$. We conclude that the KT deconfined plasma phase becomes unstable at this temperature. Note that from the inset plots of Fig. 2, one has that $\frac{\partial \mathcal{F}}{\partial T}|_{T \rightarrow T_u}$ is finite while $\frac{\partial \mathcal{E}}{\partial T}|_{T \rightarrow T_u}$ diverges. This divergency in the change of the energy density is responsible for the vanishing of the speed of sound.

To summarize, the KT black hole is dual to the chirally symmetric deconfined phase of the cascading gauge theory. This is the thermodynamically dominant phase of the theory at high temperatures. As its temperature decreases, we reach a critical point where its pressure (free energy)

first vanishes and then becomes negative (positive). At this critical temperature (2.19), a first-order deconfinement/confinement phase transition occurs. This is a nonperturbative phase transition since it proceeds via the nucleation of bubbles of the confined phase. Below this temperature, the KT deconfined chiral symmetric phase is still a metastable phase of the system all the way down to $T_u = 0.8749(0)T_c$, where it joins a perturbatively unstable branch (red dots in the plots) of the theory with negative specific heat.

There is another property of the black hole that is particularly important for our study. The KT black hole

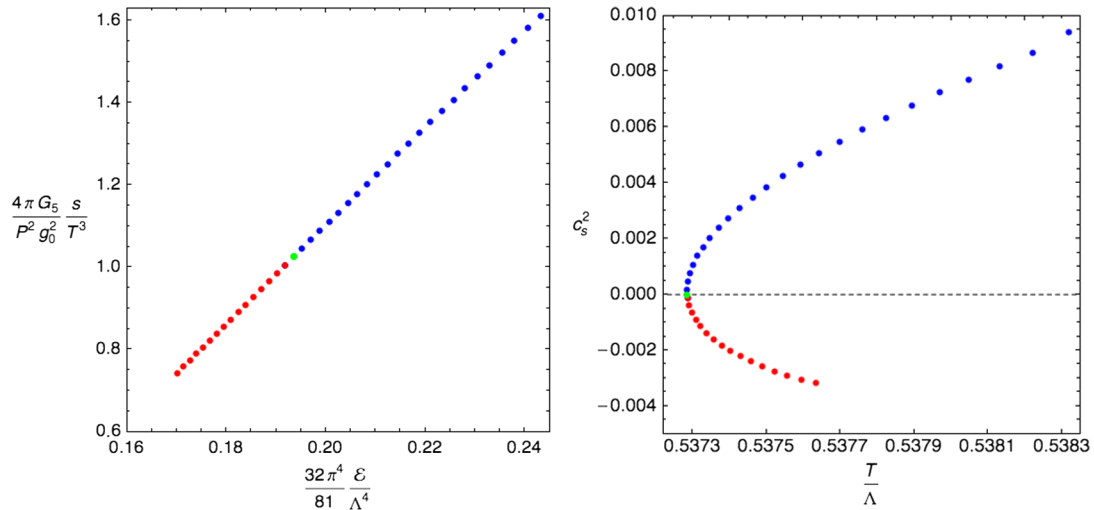


FIG. 3 (color online). *Left Panel:* The dimensionless entropy density as a function of the dimensionless energy density in the vicinity of $T = T_u$. *Right Panel:* Square of speed of sound c_s^2 in the vicinity of $T = T_u$.

is also characterized by its D5-brane and D3-brane charges. The (Maxwell) D5-brane charge, also called the fractional D3-brane charge, is simply

$$Q_{D5}^{\text{Max}} = M = \frac{2^{3/4} \pi}{3G_5^{1/4}} P, \quad (2.22)$$

where we used (2.4). The definition of the D3-brane charge is more subtle since the logarithm dependence of the fields makes a naive definition diverge, and we need a suitable regularization procedure. For a supergravity solution with nontrivial Wess-Zumino terms, one can define three different types of charges [39,40] that we now discuss. For a solution asymptoting to the KT background and with a horizon, the dimensionless D3-Page charge is ($\alpha' \equiv 1$) [6]

$$Q_{D3}^{\text{Page}} = \frac{1}{(4\pi^2)^2} \int_{T^{1,1}} (\mathcal{F}_5 - B_2 \wedge F_3), \quad (2.23)$$

where the integration is done over the $T^{1,1}$. The D3-Page charge is conserved and is independent of the radius at which it is evaluated.

We can also define the Maxwell D3 charge of the solution as

$$Q_{D3}^{\text{Max}} = \frac{1}{(4\pi^2)^2} \int_{T_{x_c}^{1,1}} \mathcal{F}_5, \quad (2.24)$$

where the integral is again performed over $T^{1,1}$, but this time with the integrand evaluated at a certain cutoff, $x = x_c$. There are two physically distinct contributions to the Maxwell charge, from the black hole (or from mobile branes when no horizon is present), Q_b , and from the charge dissolved in the fluxes (Q_f):

$$\begin{aligned} Q_{D3}^{\text{Max}} &= Q_b^{D3} + Q_f^{D3}, & Q_b^{D3} &= \frac{1}{(4\pi^2)^2} \int_{T_H^{1,1}} F_5, \\ Q_f^{D3} &= \frac{1}{(4\pi^2)^2} \left(\int_{T_{x_c}^{1,1}} F_5 - \int_{T_H^{1,1}} F_5 \right) = \frac{1}{(4\pi^2)^2} \int_{\mathcal{M}_6} H_3 \wedge F_3, \end{aligned} \quad (2.25)$$

where $\int_{T_H^{1,1}}$ means that the integrand is evaluated at the horizon $x = 1$, and \mathcal{M}_6 is the ‘‘bulk’’ spacetime spanned by the coordinates on $T^{1,1}$ plus the radial coordinate. The Maxwell charge depends on the scale at which it is measured, but if we fix a holographic screen, we expect physical processes to preserve its value at the screen. In particular, for a given scale, it must be the same if two solutions are to describe different vacua of the same theory.

For the KT black hole, we compute the Maxwell charge at the black hole horizon using (2.10) to obtain

$$Q_b^{D3} = \frac{1}{27\pi} k_0^h. \quad (2.26)$$

As described previously, the value of k_0^h is determined numerically and it is always positive, for all values of the single parameter k_s that parametrizes the KT black hole

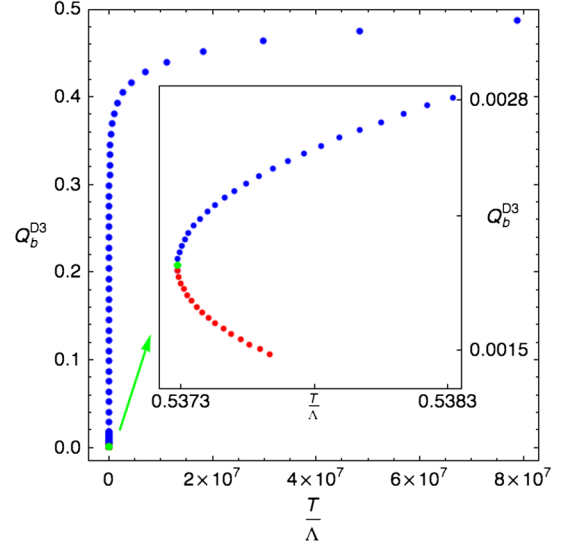


FIG. 4 (color online). The dimensionless D3-brane charge of the black hole Q_b^{D3} as a function of the dimensionless temperature.

family. Therefore, the KT black hole can only have positive Maxwell D3-brane charge at the horizon, as explicitly shown in Fig. 4. In particular, the D3 charge at the horizon Q_b^{D3} can never have opposite sign to the asymptotic D3 charge Q_{D3}^{Max} .

III. THE MASS-DEFORMED KLEBANOV-STRASSLER BLACK HOLE

A. Broken-chiral-symmetry phases of the theory: Mass-deformed cascading theories

So far we have discussed just deconfined/confined phases of the cascading gauge theory with unbroken chiral symmetry. From the holographic gauge theory perspective, the chiral symmetry preservation is explicitly manifest in the absence of expectation values for dimension-three operators in the dual thermal states. On the other hand, one knows that at zero temperature the cascading gauge theory confines into a chiral-symmetry-breaking (χ SB) phase, with the supergravity dual of this phase being the Klebanov-Strassler (KS) warped deformed conifold solution [1]. In the UV region, this solution asymptotes to the KT solution, but deep into the IR bulk, the Z_{2M} chiral symmetry is spontaneously broken to Z_2 (by gaugino condensation in the pure SYM limit of the theory) and the KS solution also breaks the $U(1)_B$ symmetry, while preserving the $SU(2) \times SU(2)$ symmetry. If we heat the theory, the confined phase persists: we have now a thermal gas of hadrons described by the KS solution with a thermal identification. A question that immediately emerges is then whether this theory also allows for the existence of a finite-temperature deconfined phase, this time with broken chiral symmetry, which we would naturally call a KS black hole. This question does not come alone. *A priori*

there is no reason for this confinement/deconfinement phase transition of the broken-chiral-symmetry phases to occur at the same critical temperature T_c —see (2.19)—of the phase transition for the chiral symmetric phases.

In supersymmetric gauge theories, chiral symmetry breaking necessarily occurs at a temperature at least as high as the confinement temperature. The question remains concerning the thermal competition of the two deconfined phases: what is the critical temperature, $T_{\chi\text{SB}}$, at which the KT black hole would exchange dominance in the partition function with the KS black hole? That is, what would be the relation between the critical temperatures for the confinement/deconfinement and the broken-/unbroken-chiral-symmetry phase transitions?

These questions were analyzed in detail in Ref. [38], whose conclusions we summarize next. We will soon realize that some of the above-described intuition needs to be reevaluated. Consider first the KT deconfined phase with unbroken chiral symmetry. A good way to learn whether this phase can condensate into a broken chiral symmetric phase is to study chiral-symmetry-breaking (χSB) deformations of this phase. In the supergravity description this amounts to study linearized gravitational perturbations about the KT black hole solution that break the chiral symmetry of the background. To make our life easier we want to restrict to the simplest sector of perturbations that break the desired symmetries while keeping frozen the fluctuations of fields irrelevant for the discussion. Reference [38] found this sector of deformations that solves the linearized equations of motion of the system. The boundary conditions further constrain the quasinormal mode spectrum of frequencies. The key observation is that the imaginary part of this frequency spectrum changes sign at a critical temperature,

$$T_{\chi\text{SB}} = 0.882503(0)T_c > T_u. \quad (3.1)$$

Actually this χSB instability is a Gregory-Laflamme type of instability, since it requires the breaking of the translational invariance along the planar spatial directions transverse to $T^{1,1}$.⁷ We seem to have all the ingredients to expect a new branch of black holes in a phase diagram of solutions of the theory. That is, at the threshold of χSB instability, we expect a natural merger of the KT black hole with what would be the KS black hole. This is where the above intuition proves to be dramatically wrong. Indeed, Ref. [38] numerically searched for gravitational solutions describing the homogeneous and isotropic states of the cascading plasma with spontaneously broken chiral symmetry. The idea was to construct the KS black hole by deforming the chirally symmetric KT black hole for

$T < T_{\chi\text{SB}}$ along the tachyonic directions revealed in the linearized analysis. This attempt was unsuccessful: there are *no* KS black hole solutions in the cascading gauge theory.

At this point, we still need to add a twist to the story. So far, we have been silently assuming that the KS deconfined phase we were searching for was breaking the chiral symmetry spontaneously. If we are less demanding, we can still search for thermal deconfined phases of the mass-deformed cascading gauge theory that explicitly break the chiral symmetry. To get the mass-deformed cascading gauge theory, one introduces the mass terms

$$\mu_i \equiv \frac{m_i}{\Lambda}, \quad i = 1, 2 \quad (3.2)$$

for the gauginos (the $\mathcal{N} = 1$ fermionic superpartners of $SU(N + M) \times SU(N)$ gauge bosons). These mass terms explicitly break both the supersymmetry and the chiral symmetry, and the theory does have a homogeneous and isotropic deconfined thermal phase. The mass terms (3.2) are the couplings of the two dimension-three operators that explicitly break the chiral symmetry,

$$\mathcal{O}_3^j = \mathcal{O}_3^j(\mu_i), \quad j = 1, 2, \quad (3.3)$$

and, in the chiral limit $\mu_i \rightarrow 0$, the expectation values for the condensates vanish as well,

$$\lim_{\mu_i \rightarrow 0} \mathcal{O}_3^j(\mu_i) = 0. \quad (3.4)$$

In the supergravity description, the homogeneous and isotropic deconfined broken chiral phase is described by what we call the mass-deformed KS black hole. This black hole was numerically constructed at the full nonlinear level in Ref. [38]. It is reassuring that the same numerical code that does not find the KS black hole dual to what would be a spontaneously broken chiral symmetric deconfined phase of the theory ($\mu_i = 0$), does find the mass-deformed KS black hole ($\mu_i \neq 0$). This definitely guarantees that the statement that KS black holes do not exist is not a consequence of a somehow incomplete numerical search.

We can now turn back to the linearized study of the χSB physical excitations of the KT black hole. The original study of Ref. [38] included linearized perturbations with the mass deformations turned on [these mass deformations are dimension-three operators and can be read from the coefficients of the non-normalizable modes that decay asymptotically as $1/r$; their normalizable partners give the VEVs for these dimension-three operators (3.3)]. This study finds that at $T = T_{\chi\text{SB}}$, the KT black hole becomes linearly unstable. As described below, the threshold of this instability signals a branch-off to a mass-deformed KS black hole in a phase diagram of solutions of the cascading theory. However, if $\mu_i = 0$, the KT black hole is still unstable but there is no associated KS black hole. The chiral limit (3.4) suggests that in this black hole background the “chiral tachyons” condensate with finite momentum: the

⁷As an interesting side note, recall that the deconfined KT plasma is thermodynamically stable down to T_u and the fact that the χSB Gregory-Laflamme instability occurs at $T_{\chi\text{SB}} > T_u$ provides an explicit example of a violation of the Gubser-Mitra conjecture.

resulting merging phase (and eventual endpoint state in a time evolution) cannot be a homogeneous and isotropic geometry described by what would be the KS black hole.

B. The mass-deformed Klebanov-Strassler black hole

In this section we will briefly review the numerical construction of the mass-deformed KS black hole [38]. This black hole describes the high-temperature phase of the mass-deformed KS theory. The zero temperature phase of this theory is dual to the Kuperstein-Sonnenschein perturbative solution [41] when the gaugino masses are equal and to the more general perturbative solution of Refs. [6,14] when the masses are arbitrary. The infrared expansion of the zero-temperature solution is included in the class of perturbative IR solutions constructed in Refs. [8,42]. Our purpose is to calculate the D3-brane charge at the horizon of the black hole in this theory and to see whether the sign of the black hole charge could somehow be made negative by scanning through the possible ranges of gaugino masses.

We are interested in the most general field ansatz of the cascading gauge theory that describes its homogeneous and isotropic states, both at zero and nonzero temperature. Such ansatz is tailored to search for the (mass-deformed) KS black holes and naturally describes also the supersymmetric Klebanov-Strassler (KS) warped deformed conifold solution [1]. It also includes as special cases the KT black hole solution and the KT singular supersymmetric solution discussed in the previous section, which further obey the constraints imposed by requiring the Z_{2M} chiral and $U(1)_B$ symmetries. In the Einstein frame this ansatz is

$$\begin{aligned} ds_{10}^2 &= g_{\mu\nu}(y)dy^\mu dy^\nu + ds_{T^{1,1}}^2, \\ ds_{T^{1,1}}^2 &= \Omega_1^2(y)g_5^2 + \Omega_2^2(y)[g_3^2 + g_4^2] + \Omega_3^2(y)[g_1^2 + g_2^2] \end{aligned} \quad (3.5)$$

for the gravitational field (y denotes the coordinates of \mathcal{M}_5 with greek indices $\mu, \nu = 0, \dots, 4$) and

$$\begin{aligned} B_2 &= h_1(y)g_1 \wedge g_2 + h_3(y)g_3 \wedge g_4, \\ F_3 &= \frac{1}{9}Pg_5 \wedge g_3 \wedge g_4 + h_2(y)(g_1 \wedge g_2 - g_3 \wedge g_4) \wedge g_5 \\ &\quad + (g_1 \wedge g_3 + g_2 \wedge g_4) \wedge d(h_2(y)), \\ F_5 &= \mathcal{F}_5 + \star \mathcal{F}_5, \\ \mathcal{F}_5 &= \left[4\Omega_0 + h_2(y)(h_3(y) - h_1(y)) + \frac{1}{9}Ph_1(y) \right] g_5 \\ &\quad \wedge g_3 \wedge g_4 \wedge g_1 \wedge g_2, \\ \Phi &= \Phi(y) \end{aligned} \quad (3.6)$$

for the fluxes $H_3 \equiv dB_2, F_3, F_5$, and dilaton Φ . P is again an integer corresponding to the RR 3-form flux on the compact 3-cycle (and to the number of fractional branes on the conifold), as given in (2.4).

To make closer contact with the original study of the KS warped deformed conifold [1], we use the 1-forms on $T^{1,1}$,

$$\begin{aligned} g_1 &= \frac{\alpha^1 - \alpha^3}{\sqrt{2}}, & g_2 &= \frac{\alpha^2 - \alpha^4}{\sqrt{2}}, & g_3 &= \frac{\alpha^1 + \alpha^3}{\sqrt{2}}, \\ g_4 &= \frac{\alpha^2 + \alpha^4}{\sqrt{2}}, & g_5 &= \alpha^5, \end{aligned} \quad (3.7)$$

where

$$\begin{aligned} \alpha^5 &= d\psi + \cos\theta_1 d\phi_1 + \cos\theta_2 d\phi_2, \\ \alpha^1 &= -\sin\theta_1 d\phi_1, & \alpha^2 &= d\theta_1, \\ \alpha^3 &= \cos\psi \sin\theta_2 d\phi_2 - \sin\psi d\theta_2, \\ \alpha^4 &= \sin\psi \sin\theta_2 d\phi_2 + \cos\psi d\theta_2, \end{aligned} \quad (3.8)$$

instead of those in (2.3).

With this ansatz, a Kaluza-Klein reduction of the type IIB action to five dimensions yields the effective action [38],

$$\begin{aligned} S_5 &= \frac{108}{16\pi G_5} \int_{\mathcal{M}_5} \text{vol}_{\mathcal{M}_5} \Omega_1 \Omega_2^2 \Omega_3^2 \left\{ R_{10} - \frac{1}{2}(\nabla\Phi)^2 \right. \\ &\quad - \frac{1}{2}e^{-\Phi} \left(\frac{(h_1 - h_3)^2}{2\Omega_1^2 \Omega_2^2 \Omega_3^2} + \frac{1}{\Omega_3^4}(\nabla h_1)^2 + \frac{1}{\Omega_2^4}(\nabla h_3)^2 \right) \\ &\quad - \frac{1}{2}e^{\Phi} \left(\frac{2}{\Omega_2^2 \Omega_3^2}(\nabla h_2)^2 + \frac{1}{\Omega_1^2 \Omega_2^4} \left(h_2 - \frac{P}{9} \right)^2 + \frac{1}{\Omega_1^2 \Omega_3^4} h_2^2 \right) \\ &\quad \left. - \frac{1}{2\Omega_1^2 \Omega_2^4 \Omega_3^4} \left(4\Omega_0 + h_2(h_3 - h_1) + \frac{1}{9}Ph_1 \right)^2 \right\}, \end{aligned} \quad (3.9)$$

where R_{10} is given in terms of the five-dimensional Ricci scalar of the metric $g_{\mu\nu}$ as

$$\begin{aligned} R_{10} &= R_5 + \left(\frac{1}{2\Omega_1^2} + \frac{2}{\Omega_2^2} + \frac{2}{\Omega_3^2} - \frac{\Omega_2^2}{4\Omega_1^2 \Omega_3^2} - \frac{\Omega_3^2}{4\Omega_1^2 \Omega_2^2} - \frac{\Omega_1^2}{\Omega_2^2 \Omega_3^2} \right) \\ &\quad - 2\Box_5 \ln(\Omega_1 \Omega_2^2 \Omega_3^2) - \{ (\nabla \ln \Omega_1)^2 + 2(\nabla \ln \Omega_2)^2 \\ &\quad + 2(\nabla \ln \Omega_3)^2 + (\nabla \ln(\Omega_1 \Omega_2^2 \Omega_3^2))^2 \}, \end{aligned} \quad (3.10)$$

and ∇ and \Box_5 denote the covariant derivative and the Laplacian in \mathcal{M}_5 , respectively. This action (3.9) also describes the theory governed by (2.5) as a special limit [38].

The general five-dimensional background geometry with homogeneous and isotropic (but not necessary Lorentz-invariant) asymptotic boundary takes the form written in (2.8). It is tailored to search for the (mass-deformed) KS black hole with horizon located at $x = 1$ and asymptotic KT background at $x \rightarrow 0$. It is also useful to encode all the information convening the warp-squashed $T^{1,1}$ factors $\Omega_{1,2,3}(x)$, the flux-form functions $h_{1,2,3}(x)$ and the dilaton $\Phi(x)$ in the following set of new functions $\{K_1, K_2, K_3, f_a, f_b, f_c, h, g\}$ defined as

$$\begin{aligned}
 \Omega_i &= \omega_i H^{1/4} \quad (i = 1, 2, 3), \quad H(x) = (2x - x^2)h(x), \\
 \omega_1(x) &= \frac{\sqrt{f_c(x)}}{3(2x - x^2)^{1/4}}, \quad \omega_2(x) = \frac{\sqrt{f_a(x)}}{\sqrt{6}(2x - x^2)^{1/4}}, \\
 \omega_3(x) &= \frac{\sqrt{f_b(x)}}{\sqrt{6}(2x - x^2)^{1/4}}; \quad h_1(x) = \frac{1}{P} \left(\frac{1}{12} K_1(x) - 36\Omega_0 \right), \\
 h_2(x) &= \frac{P}{18} K_2(x), \quad h_3(x) = \frac{1}{P} \left(\frac{1}{12} K_3(x) - 36\Omega_0 \right); \\
 g(x) &= e^{\Phi(x)}. \tag{3.11}
 \end{aligned}$$

From the equations of motion of (3.9), we find that $G_{xx}(x)$ can be expressed by an algebraic relation that is a function of $\{K_1, K_2, K_3, f_a, f_b, f_c, h, g\}$ and their first derivatives. The nontrivial equations of motion can then be written as a system of eight second-order nonlinear coupled ODEs for $\{K_1, K_2, K_3, f_a, f_b, f_c, h, g\}$. Each of these eight equations is second order. It follows that the total differential order of the system is 16. The constant Ω_0 , introduced in (3.6), does not appear in the equations of motion.

The (mass-deformed) KS black hole must solve these equations of motion subject to appropriate boundary conditions at the horizon, $x \rightarrow 1$, and at the asymptotic boundary, $x \rightarrow 0$.

$$\begin{aligned}
 K_1 &= 4h_0 a_0^2 - \frac{1}{2} P^2 g_0 - \frac{1}{2} P^2 g_0 \ln x + \sum_{n=1}^{\infty} \sum_k k_{1nk} x^{n/4} \ln^k x, & K_2 &= 1 + \sum_{n=1}^{\infty} \sum_k k_{2nk} x^{n/4} \ln^k x, \\
 K_3 &= 4h_0 a_0^2 - \frac{1}{2} P^2 g_0 - \frac{1}{2} P^2 g_0 \ln x + \sum_{n=1}^{\infty} \sum_k k_{3nk} x^{n/4} \ln^k x, & f_\alpha &= a_0 \left(1 + \sum_{n=1}^{\infty} \sum_k f_{\alpha nk} x^{n/4} \ln^k x \right), \quad \alpha = \{a, b\} \\
 f_c &= a_0 \left(1 + \sum_{n=2}^{\infty} \sum_k f_{cnk} x^{n/4} \ln^k x \right), & h &= h_0 - \frac{P^2 g_0}{8a_0^2} \ln x + \sum_{n=2}^{\infty} \sum_k h_{nk} x^{n/4} \ln^k x, & g &= g_0 \left(1 + \sum_{n=2}^{\infty} \sum_k g_{nk} x^{n/2} \ln^k x \right). \tag{3.14}
 \end{aligned}$$

There are six independent microscopic parameters. Four of them describe the KT solution, namely $\{P, g_0, a_0, h_0\}$, and have exactly the physical interpretation already described below (3.14). In particular, h_0 can be traded for the dimensionless parameter k_s , defined in (2.13), which defines the dynamical scale Λ of the cascading theory. Moreover, the straightforward extension (to accommodate for the field content of the KS ansatz) of the three scaling symmetries discussed in (2.14) and (2.15) still allows us to set

$$P = g_0 = a_0 \equiv 1. \tag{3.15}$$

The other two independent microscopic parameters are $\{k_{110}, f_{a10}\}$ and are related to the couplings of the two dimension-three operators that explicitly break the chiral symmetry. The explicit relation between $\{k_{110}, f_{a10}\}$ and these two mass-deformation parameters $\{\mu_1, \mu_2\}$ of the cascading gauge theory introduced in (3.2) is

Near the horizon, ($x \rightarrow 1$), the equations of motion have the IR series expansion,

$$\begin{aligned}
 K_i &= \sum_{n=0}^{\infty} k_{in}^h (1-x)^{2n}, \quad i = 1, 2, 3, \\
 f_\alpha &= a_0 \sum_{n=0}^{\infty} f_{\alpha n}^h (1-x)^{2n}, \quad \alpha = a, b, c, \\
 h &= \sum_{n=0}^{\infty} h_n^h (1-x)^{2n}, \quad g = g_0 \sum_{n=0}^{\infty} g_n^h (1-x)^{2n}. \tag{3.12}
 \end{aligned}$$

and regularity of the expansion in the ingoing Eddington-Finkelstein coordinates requires the leading terms of this expansion to be just regular. There are nine independent IR parameters that we choose to be,

IR independent parameters (9):

$$\{k_{1h0}, k_{2h0}, k_{3h0}, f_{ah0}, f_{ah1}, f_{bh0}, f_{ch0}, h_{h0}, g_{h0}\}. \tag{3.13}$$

At the UV asymptotic boundary we want the (mass-deformed) KS black hole to asymptote to the KT solution [2], while allowing also for the mass-deformation parameters. The latter is the leading-order contribution of a power series expansion in x and $\ln(x)$ of the equations of motion,

$$\begin{aligned}
 f_{a10} &= (\mu_1 + 4\mu_2 k_s) e^{-k_s/2}, \\
 \left(k_{110} + \frac{1}{2} P^2 g_0 f_{a10} \right) (3P^2 g_0 + 8h_0 a_0^2)^{-1} &= \mu_2 e^{-k_s/2}. \tag{3.16}
 \end{aligned}$$

In addition to these microscopic UV parameters, there are seven extra independent parameters $\{f_{a30}, k_{230}, f_{a40}, g_{40}, f_{a60}, f_{a70}, f_{a80}\}$ associated with the VEVs of the operators dual to the fields for which we are solving. Summarizing, after using the scaling symmetries of our system, we are left with ten UV independent parameters,

UV independent parameters (10):

$$\{k_s, k_{110}, f_{a10}, f_{a30}, k_{230}, f_{a40}, g_{40}, f_{a60}, f_{a70}, f_{a80}\}. \tag{3.17}$$

The total number of IR and UV independent parameters is $9 + 10 = 19$ and is given by (3.13) and (3.17). On the other hand, the equations of motion are a system of total differential order 16. Therefore, a general mass-deformed KS black hole is a three-parameter family of solutions. We naturally take these three parameters to be the microscopic parameters of the cascading gauge theory, namely $\{k_s, k_{110}, f_{a10}\}$. We can then use (2.13) and (3.16) to express the results in terms of the temperature T/Λ and the mass-deformation parameters $\{\mu_1, \mu_2\}$. Of course, if we are just interested in the KS black hole that would describe the spontaneously symmetry-broken deconfined phase, we set $\mu_1 = \mu_2 = 0$, and we have simply a one-parameter family of solutions. As emphasized previously, the numerical code does find generic mass-deformed KS black holes (whose properties will be discussed below), but when we crank down the mass deformations to zero, no solution with $\mathcal{O}_3^j \neq 0$ is found.

The numerical construction of the mass-deformed KS black holes is done using a shooting method similar to the one used in the construction of the KT black hole. In this shooting method, the IR power series solution (3.12) is constructed up to order $n = 1$ (inclusive), and the asymptotic UV series solution (3.14) is constructed up to eighth order ($n = 8$, inclusive). One then evolves these solutions away from these critical points and does the matching in the overlapping intermediate region (at $x = 0.5$). Fixing the microscopic parameters $\{k_s, k_{110}, f_{a10}\}$, we still have 16 independent IR/UV parameters that are determined by the 16 conditions that follow from requiring that the eight functions $\{K_1, K_2, K_3, f_a, f_b, f_c, h, g\}$ and their first derivatives are continuous at $x = 0.5$. The process is repeated for different values of $\{k_s, k_{110}, f_{a10}\}$.

C. Properties of the mass-deformed Klebanov-Strassler black hole

Two quantities of utmost interest for our discussion are the D5-brane and D3-brane charges of the mass-deformed KS black hole. The former is simply given by (2.22), $Q_{D5}^{\text{Max}} = M$. On the other hand, we can compute the Maxwell D3 charge of the black hole (2.25) using (3.12) to get

$$Q_b^{D3} = \frac{k_{10}^h(2 - k_{20}^h) + k_{20}^h k_{30}^h}{54\pi}. \quad (3.18)$$

Note that the constant Ω_0 introduced in (3.6) does not appear in the equations of motion nor in the flux F_5 , but it does appear in the contribution $B_2 \wedge F_3$ to the D3-Page charge (2.23). Below we present the properties of the mass-deformed KS black hole solution. As described above, this is a three-parameter family of solutions parametrized by $\{k_s, k_{110}, f_{a10}\}$, the values of which we give as an input to the code. The values of $\{k_{10}^h, k_{20}^h, k_{30}^h\}$ are then determined numerically. For the several families of values of

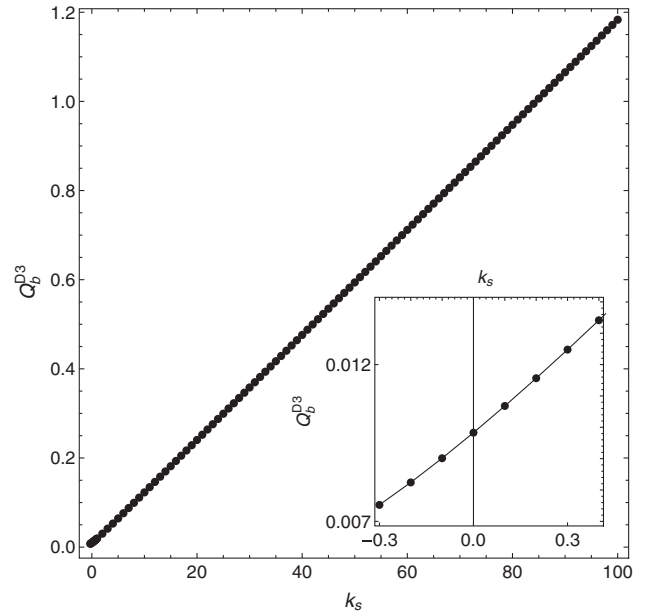


FIG. 5. Mobile D3-brane charge Q_b^{D3} for mass-deformed KS black holes with mass-deformation parameters $f_{a10} = 0.1$ and $k_{110} = 0$, as a function of k_s (related to T/Λ).

$\{k_s, k_{110}, f_{a10}\}$ that we have tried, it is always true that $Q_b^{D3} > 0$.

We outline now our searches. In Fig. 5 we present values of Q_b^{D3} with mass-deformation parameters $f_{a10} = 0.1$ and $k_{110} = 0$, as a function of k_s (related to T/Λ). Note that smaller values of k_s bring down the Maxwell D3-brane charge at the horizon; it is thus desirable to study the smallest possible values of k_s . The technical reason that restricts this is rooted in the instability of the finite-difference codes⁸ used to simulate mass-deformed KS black holes for small k_s . The insert in Fig. 5 shows the smallest values of k_s we can trust with our current numerics. A quadratic fit (in k_s) to these eight points shows that

$$\min_{k_s} [Q_b^{D3}(f_{a10} = 0.1, k_{110} = 0; k_s)] = 0.000323195. \quad (3.19)$$

Figures 6 and 7 present the results of a different search strategy. Namely, we fix k_s (set $k_s = 0$ for Fig. 6 and $k_s = -0.5$ for Fig. 7) and generate families of mass-deformed KS black holes by scanning the mass-deformation parameter k_{110} for a discrete set of $f_{a10} = \{-0.4, \dots, 0.4\}$ (see the left panels). For each of these curves we use quadratic extrapolation to determine $\min_{k_{110}} [Q_b^{D3}]$ (see the right panels). Finally, Fig. 8 indicates functional relations between non-normalizable modes f_{a10} and k_{110} at minima of Q_b^{D3} for $k_s = 0$ (see the left panel) and $k_s = -0.5$ (see the right panel). The solid green lines represent the best linear fit $k_{110} \propto f_{a10}$. Note that (3.16) implies

⁸It is possible that these instabilities can be alleviated with spectral methods. We hope to report on this in future work.

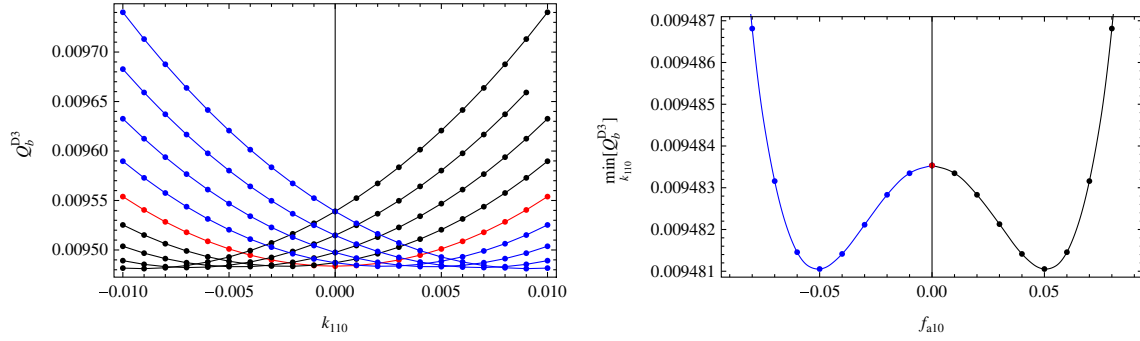


FIG. 6 (color online). *Left Panel:* Mobile D3-brane charge Q_b^{D3} for mass-deformed KS black holes with parameters $k_s = 0$ and $f_{a10} = \{-0.4, \dots, 0.4\}$, as a function of the mass-deformation parameter k_{110} . The central red curve/dots (fourth line from bottom/left) with minimum at $k_{110} = 0$ is for $f_{a10} = 0$. As f_{a10} grows increasingly positive, the minimum shifts to the left (the first four black curves on the left bottom corner are for $f_{a10} = \{0.1, \dots, 0.4\}$). As f_{a10} grows increasingly negative, the minimum shifts to the right (the last four blue curves on the left are for $f_{a10} = \{-0.4, \dots, -0.1\}$). *Right Panel:* Minima of the black hole D3-brane charge Q_b^{D3} for mass-deformed KS black holes with respect to k_{110} for $k_s = 0$, as a function of the mass-deformation parameter f_{a10} .

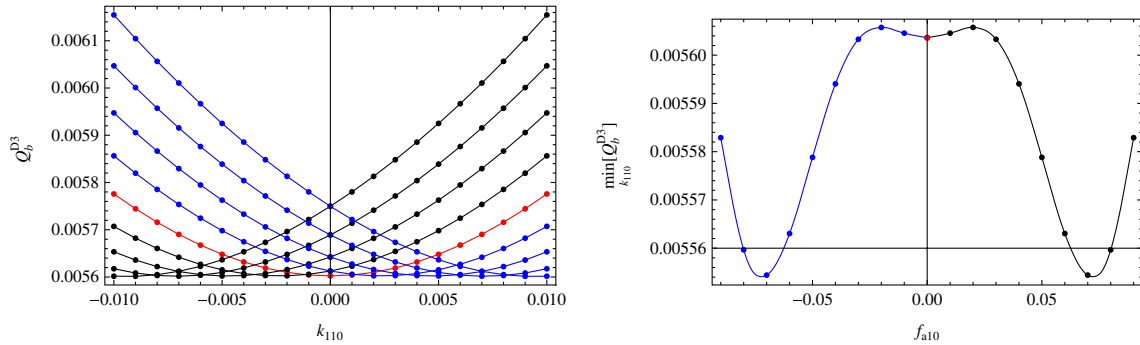


FIG. 7 (color online). Same as Fig. 6, but with $k_s = -0.5$.

$$k_{110} = f_{a10} \frac{4\mu_2 - \frac{\mu_1}{2}}{\mu_1 + 4\mu_2 k_s}. \quad (3.20)$$

Thus, a linear relation between k_{110} and f_{a10} , if true, would imply a linear relation between m_1 and m_2 . From the fits we determine

$$\frac{m_2}{m_1} = \begin{cases} 0.072, & \text{for } k_s = 0; \\ 0.064, & \text{for } k_s = -0.5. \end{cases} \quad (3.21)$$

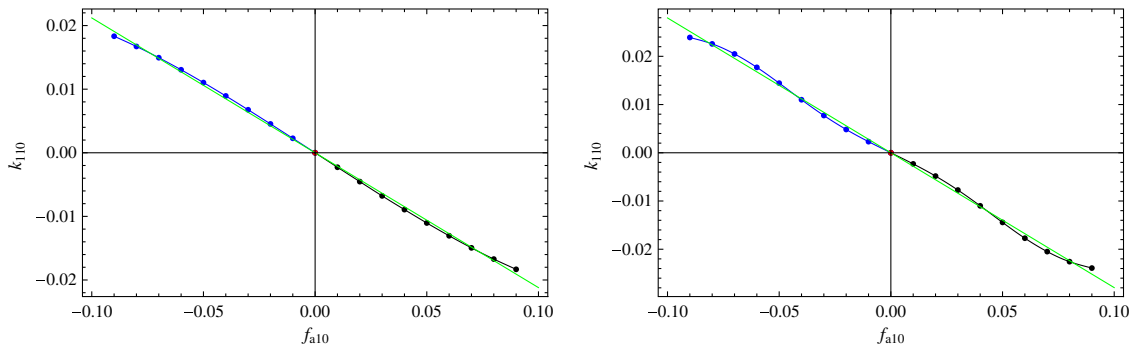


FIG. 8 (color online). Relation between the mass-deformation parameters f_{a10} and k_{110} for $k_s = 0$ (*Left Panel*) and $k_s = -0.5$ (*Right Panel*) at $\min Q_b^{D3}$. The solid green lines represent the best-fit linear relation $f_{a10} \propto k_{110}$.

Assuming that discrepancy between $\frac{m_2}{m_1}$ for different k_s is a numerical artifact, an interesting question remains as to the physical significance of this ratio.

Although we cannot exclude the possibility that there is some region in the parameter space that yields $Q_b^{D3} < 0$, we could not find it. We take this, together with the fact that the KT black hole of the previous section always has positive Q_b^{D3} (recall that for this solution we could run the full parameter space since it is a one-parameter solution),

as strong evidence for the nonexistence of KS black holes with $Q_b^{D3} < 0$. To summarize, the mass-deformed KS black holes we have examined always have positive Maxwell D3-brane charge at the horizon; there appear to be no such black holes that have a Maxwell charge whose sign is opposite to that of the asymptotic charge of the solution.

IV. CONCLUSION

The idea of a landscape of de Sitter vacua in string theory is founded on two pillars. The first is the construction of a very large number of string theory compactifications with stabilized moduli, either via the KKLT construction [9] or by another mechanism [12], which always give anti-de Sitter vacua. The second is the uplift of these vacua to de Sitter, and the most common way to do this is to trap anti-D3 branes in warped deformed conifoldlike regions of the compactification manifold [9]. The recent analysis of Refs. [4–6,8] shows that the geometries corresponding to these antibranes are singular, and that furthermore this singularity does not appear to be resolved à la Polchinski-Strassler [22], which is its most obvious resolution channel [23]; this supports the idea that this singularity is not physical and should therefore be discarded.

In this paper we have looked at the issue from a different perspective. If the singularities coming from anti-D3 branes at the bottom of the Klebanov-Strassler throat are physical, then following [28], it should be possible to cloak them with a regular Schwarzschild horizon. The resulting nonextremal geometries would be Klebanov-Tseytlin or Klebanov-Strassler black holes that have negative D3-brane Maxwell charge Q_b^{D3} at the horizon. These black holes were constructed numerically in Refs. [34,35,38], and we did an extensive scan of all these numerical solutions but were unable to find any solution with $Q_b^{D3} < 0$. While not a rigorous proof, our negative result strongly supports the idea that singularities generated by anti-D3 branes at the bottom of the warped deformed conifold are unphysical. This in turn suggests that the most common mechanism for uplifting the landscape of AdS vacua obtained from string theory compactifications with stabilized moduli to deSitter does not work, and hence string theory may only have a landscape of AdS vacua but not a landscape of deSitter vacua.

Furthermore, we also found that the charge of a given KT or mass-deformed KS black hole is not an independent parameter but is completely determined by the temperature

and the gaugino masses. This implies that if one is to perform a gedanken experiment that consists of lowering an anti-D3 brane into this black hole keeping the temperature fixed, the charge of this black hole will become a bit smaller for a moment but then will immediately go back to its previous value by absorbing charge from the surrounding fluxes. Hence, this black hole acts as a catalyst for brane-charge annihilation for arbitrarily small values of the temperature, and this may suggest that adding an antibrane to a vacuum Klebanov-Strassler solution will cause the surrounding flux to immediately annihilate it [43].

It would be interesting to further push the limits of the KT/KS black hole parameter space (driven by the development of more efficient numerical techniques) in order to establish more completely that regular nonextremal geometries with $Q_b^{D3} < 0$ do not exist. It would also be interesting to compute D3-brane charge of the bottom of de Sitter deformed KT/KS geometries [44,45]. We hope to report on this in future work.

ACKNOWLEDGMENTS

It is a pleasure to thank Gregory Giecold, Mariana Graña, Stanislav Kuperstein, Stefano Massai, Al Muller, Jorge Santos and Thomas van Riet for interesting and helpful discussions. This work was supported in part by the ANR Grant No. 08-JCJC-0001-0, the ERC Starting Grant No. 240210, String-QCD-BH, and by NSERC Discovery Grants. Research at Perimeter Institute is supported by the Government of Canada through Industry Canada and by the Province of Ontario through the Ministry of Research and Innovation. A.B. and O.J.C.D. would like to thank the Institut de Physique Théorique, CEA-Saclay and the Perimeter Institute, respectively, for hospitality during various stages of this work. O.J.C.D. further thanks the Yukawa Institute for Theoretical Physics (YITP) at Kyoto University, where part of this work was completed during the YITP-T11-08 programme “Recent advances in numerical and analytical methods for black hole dynamics,” and, for discussions, the participants of the following workshops: The Holographic Way: String Theory, Gauge Theory and Black Holes at Nordita, Spanish Relativity Meeting in Portugal, Exploring AdS-CFT Dualities in Dynamical Settings at the Perimeter Institute and Holography, Gauge Theory and Black Holes at IOP Amsterdam for discussions.

-
- [1] I. R. Klebanov and M. J. Strassler, *J. High Energy Phys.* **08** (2000) 052.
 [2] I. R. Klebanov and A. A. Tseytlin, *Nucl. Phys.* **B578**, 123 (2000).

- [3] S. Kachru, J. Pearson, and H. L. Verlinde, *J. High Energy Phys.* **06** (2002) 021.
 [4] I. Bena, M. Grana, and N. Halmagyi, *J. High Energy Phys.* **09** (2010) 087.

- [5] I. Bena, G. Giecold, M. Grana, N. Halmagyi, and S. Massai, *Classical Quantum Gravity* **30**, 015003 (2013).
- [6] I. Bena, G. Giecold, M. Grana, N. Halmagyi, and S. Massai, [arXiv:1106.6165](https://arxiv.org/abs/1106.6165).
- [7] S. Massai, [arXiv:1202.3789](https://arxiv.org/abs/1202.3789).
- [8] I. Bena, M. Grana, S. Kuperstein, and S. Massai, [arXiv:1206.6369](https://arxiv.org/abs/1206.6369).
- [9] S. Kachru, R. Kallosh, A. D. Linde, and S. P. Trivedi, *Phys. Rev. D* **68**, 046005 (2003).
- [10] A. Saltman and E. Silverstein, *J. High Energy Phys.* **11** (2004) 066.
- [11] O. Lebedev, H. P. Nilles, and M. Ratz, *Phys. Lett. B* **636**, 126 (2006).
- [12] V. Balasubramanian, P. Berglund, J. P. Conlon, and F. Quevedo, *J. High Energy Phys.* **03** (2005) 007.
- [13] M. Rummel and A. Westphal, *J. High Energy Phys.* **01** (2012) 020.
- [14] A. Dymarsky, *J. High Energy Phys.* **05** (2011) 053.
- [15] I. Bena, E. Gorbatov, S. Hellerman, N. Seiberg, and D. Shih, *J. High Energy Phys.* **11** (2006) 088.
- [16] D. Kutasov and A. Wissanji, *J. High Energy Phys.* **09** (2012) 080.
- [17] G. T. Horowitz and R. C. Myers, *Gen. Relativ. Gravit.* **27**, 915 (1995).
- [18] I. Bena, G. Giecold, and N. Halmagyi, *J. High Energy Phys.* **04** (2011) 120.
- [19] S. Massai, *J. High Energy Phys.* **06** (2012) 059.
- [20] G. Giecold, E. Goi, and F. Orsi, *J. High Energy Phys.* **02** (2012) 019.
- [21] R. C. Myers, *J. High Energy Phys.* **12** (1999) 022.
- [22] J. Polchinski and M. J. Strassler, [arXiv:hep-th/0003136](https://arxiv.org/abs/hep-th/0003136).
- [23] I. Bena, M. Grana, S. Kuperstein, and S. Massai, [arXiv:1212.4828](https://arxiv.org/abs/1212.4828).
- [24] J. Blåbäck, U. H. Danielsson, D. Junghans, T. Riet, T. Wrase, and M. Zagermann, *J. High Energy Phys.* **12** (2010) 043.
- [25] J. Blåbäck, U. H. Danielsson, D. Junghans, T. Riet, T. Wrase, and M. Zagermann, *J. High Energy Phys.* **08** (2011) 105.
- [26] J. Blaback, U. H. Danielsson, D. Junghans, T. Van Riet, T. Wrase and M. Zagermann, *J. High Energy Phys.* **02** (2012) 025.
- [27] I. Bena, D. Junghans, S. Kuperstein, T. Van Riet, T. Wrase and M. Zagermann, *J. High Energy Phys.* **10** (2012) 078.
- [28] S. S. Gubser, *Adv. Theor. Math. Phys.* **4**, 679 (2000).
- [29] A. Buchel, *Nucl. Phys.* **B600**, 219 (2001).
- [30] I. R. Klebanov and E. Witten, *Nucl. Phys.* **B536**, 199 (1998).
- [31] A. Buchel, C. P. Herzog, I. R. Klebanov, L. A. Pando Zayas and A. A. Tseytlin, *J. High Energy Phys.* **04** (2001) 033.
- [32] S. S. Gubser, C. P. Herzog, I. R. Klebanov, and A. A. Tseytlin, *J. High Energy Phys.* **05** (2001) 028.
- [33] O. Aharony, A. Buchel, and A. Yarom, *Phys. Rev. D* **72**, 066003 (2005).
- [34] O. Aharony, A. Buchel, and P. Kerner, *Phys. Rev. D* **76**, 086005 (2007).
- [35] A. Buchel, *Nucl. Phys.* **B820**, 385 (2009).
- [36] M. Mahato, L. A. Pando Zayas and C. A. Terrero-Escalante, *J. High Energy Phys.* **09** (2007) 083.
- [37] E. Caceres, C. Nunez, and L. A. Pando-Zayas, *J. High Energy Phys.* **03** (2011) 054.
- [38] A. Buchel, *Nucl. Phys.* **B847**, 297 (2011).
- [39] D. Marolf, [arXiv:hep-th/0006117](https://arxiv.org/abs/hep-th/0006117).
- [40] O. Aharony, A. Hashimoto, S. Hirano, and P. Ouyang, *J. High Energy Phys.* **01** (2010) 072.
- [41] S. Kuperstein and J. Sonnenschein, *J. High Energy Phys.* **02** (2004) 015.
- [42] P. McGuirk, G. Shiu, and Y. Sumitomo, *Nucl. Phys.* **B842**, 383 (2011).
- [43] J. Blaback, U. H. Danielsson and T. Van Riet, *J. High Energy Phys.* **02** (2013) 061.
- [44] A. Buchel, *Phys. Rev. D* **65**, 125015 (2002).
- [45] A. Buchel, *Phys. Rev. D* **74**, 046009 (2006).